Cell Reports

Article

Tentonin 3/TMEM150C regulates glucose-stimulated insulin secretion in pancreatic β-cells

Graphical abstract

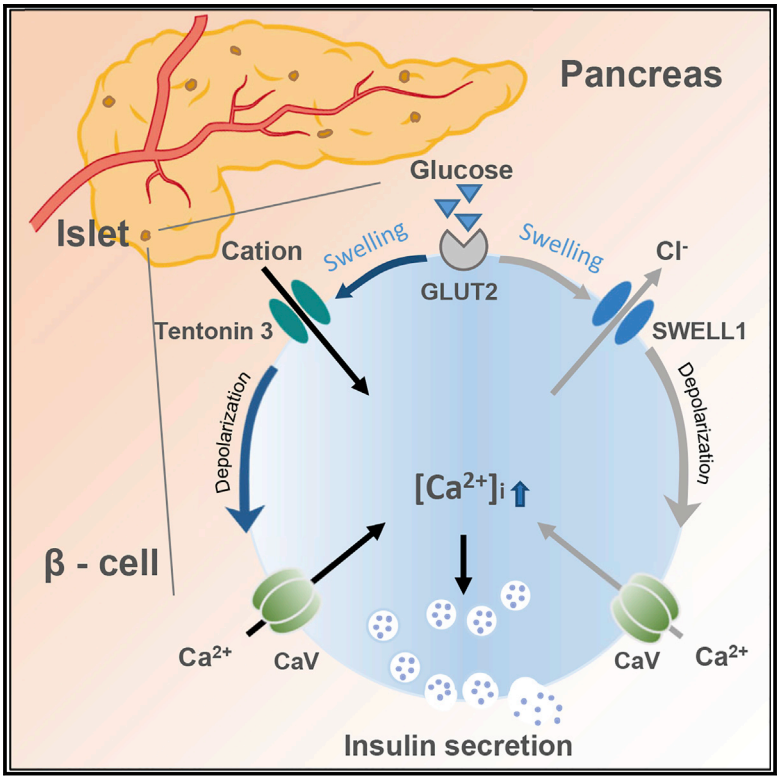

Authors

Jungwon Wee, Sungmin Pak, Tahnbee Kim, ..., Mi-Ock Lee, Kyong Soo Park, Uhtaek Oh

Correspondence

kspark@snu.ac.kr (K.S.P.), utoh@kist.re.kr (U.O.)

In brief

Wee et al. show that Tentonin 3/TMEM150C (TTN3) is a stretch-activated cation channel contributing insulin secretion induced by high glucose levels and hypotonicity. TTN3-deficient pancreatic beta cells exhibit impaired glucose-induced insulin secretion, identifying an additional regulatory pathway for diabetes mellitus.

Highlights

- Tentonin 3/TMEM150C (TTN3) is expressed specifically in murine pancreatic β-cells
- TTN3 mediates β-cell swelling upon glucose stimulation and hypotonicity
- TTN3 mediates cation current influx upon glucose stimulation and hypotonicity
- Genetic ablation of TTN3 in β-cells impairs insulin secretion by glucose

Wee et al., 2021, Cell Reports 37, 110067
November 30, 2021
https://doi.org/10.1016/j.celrep.2021.110067

CellPress

Cell Reports

CellPress
OPEN ACCESS

Article

Tentonin 3/TMEM150C regulates glucose-stimulated insulin secretion in pancreatic β-cells

Jungwon Wee,[1,4,5] Sungmin Pak,[2,4,5] Tahnbee Kim,[4] Gyu-Sang Hong,[4] Ji Seon Lee,[3] Jinyan Nan,[3] Hyungsup Kim,[4] Mi-Ock Lee,[2] Kyong Soo Park,[1,3,*] and Uhtaek Oh[1,4,6,*]

[1]Department of Molecular Medicine and Biopharmaceutical Sciences, Graduate School of Convergence Science and Technology, Seoul National University, Seoul 03080, Korea
[2]College of Pharmacy, Seoul National University, Seoul 08826, Korea
[3]Department of Internal Medicine, College of Medicine, Seoul National University, Seoul 03080, Korea
[4]Brain Science Institute, Korea Institute of Science and Technology (KIST), Seoul 02792, Korea
[5]These authors contributed equally
[6]Lead contact
*Correspondence: kspark@snu.ac.kr (K.S.P.), utoh@kist.re.kr (U.O.)
https://doi.org/10.1016/j.celrep.2021.110067

SUMMARY

Glucose homeostasis is initially regulated by the pancreatic hormone insulin. Glucose-stimulated insulin secretion in β-cells is composed of two cellular mechanisms: a high glucose concentration not only depolarizes the membrane potential of the β-cells by ATP-sensitive K^+ channels but also induces cell inflation, which is sufficient to release insulin granules. However, the molecular identity of the stretch-activated cation channel responsible for the latter pathway remains unknown. Here, we demonstrate that Tentonin 3/TMEM150C (TTN3), a mechanosensitive channel, contributes to glucose-stimulated insulin secretion by mediating cation influx. TTN3 is expressed specifically in β-cells and mediates cation currents to glucose and hypotonic stimulations. The glucose-induced depolarization, firing activity, and Ca^{2+} influx of β-cells were significantly lower in *Ttn3*$^{-/-}$ mice. More importantly, *Ttn3*$^{-/-}$ mice show impaired glucose tolerance with decreased insulin secretion *in vivo*. We propose that TTN3, as a stretch-activated cation channel, contributes to glucose-stimulated insulin secretion.

INTRODUCTION

Type 2 diabetes is a metabolic disorder characterized by impaired glucose tolerance (Kahn, 2000). Glucose homeostasis is primarily maintained by an endocrine hormone, insulin, which is secreted by pancreatic β-cells. Insulin enhances glucose storage or regulates glycogen breakdown in muscle cells, keeping the blood glucose level within a controlled range (LeRoith, 2002). When the β-cells produce an insufficient amount of insulin or when the body cannot use the insulin properly, it leads to high blood glucose levels or hyperglycemia, which is the hallmark of diabetes mellitus (Ashcroft and Rorsman, 2012; Porte and Kahn, 2001). The number of people suffering from diabetes mellitus has been rising rapidly in the past three decades. In addition, diabetes mellitus is expected to be the seventh leading cause of death in 2030 (Mathers and Loncar, 2006; Zheng et al., 2018). Moreover, it has serious complications such as blindness, neuropathy, heart attacks, stroke, and kidney failure (Zhuo et al., 2013). More than one-half of the lifetime medical costs of people in the United States have been used to treat those diabetic complications (Zhuo et al., 2013). Accordingly, development in the treatment of diabetes is important to improve one's quality of life through increasing insulin sensitivity or the amount of insulin secretion in the pancreas.

The primary pathway regulating glucose-stimulated insulin secretion is through the activity of ATP-sensitive K^+ (K_{ATP}) channels (Henquin, 2009, 2011). Extracellular glucose is transported into the β-cells by glucose transporter 2 (GLUT2) and metabolized in the mitochondria, which increases the intracellular ATP/ADP ratio (Henquin, 2011). The increased ATP level leads to the closure of the K_{ATP} channel, which in turn evokes the depolarization of β-cells (Ashcroft et al., 1984; Cook and Hales, 1984). The latter eventually activates the residing voltage-gated calcium channels, dragging in extracellular Ca^{2+} into the cytoplasm (Henquin, 2011). The increased level of cytoplasmic Ca^{2+} triggers exocytosis of insulin granules from β-cells (Henquin, 2011; MacDonald et al., 2005; Rorsman and Ashcroft, 2018).

Although the main triggering pathway for glucose-stimulated insulin secretion is the K_{ATP}-dependent pathway, the involvement of the K_{ATP}-channel-independent pathway (amplifying pathway) has also been proposed (Henquin, 2009, 2011). For example, glucose induces insulin secretion from islets lacking K_{ATP} channels (Ravier et al., 2009). One of the candidate

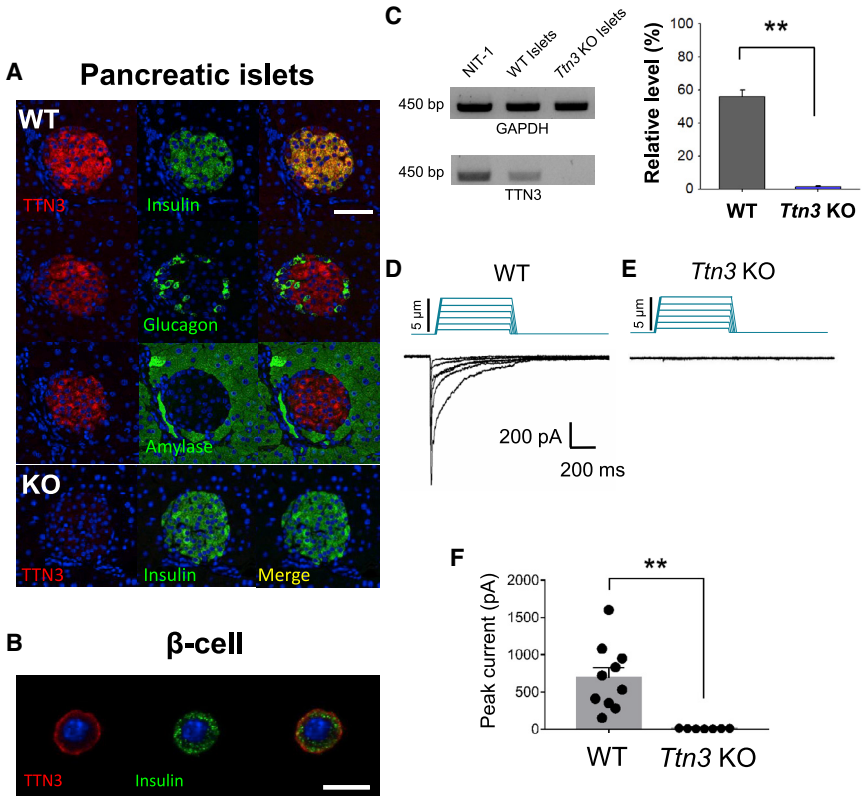

Figure 1. Tentonin 3/TMEM150C (TTN3) is expressed in β-cells in the mouse pancreas

(A) Immunofluorescence stainings of TTN3 (red) and insulin (green; top panels), glucagon (green; middle panels), or amylase (green; bottom panels) in wild-type (WT) and *Ttn3* knockout (KO) mouse pancreas sections. Scale bar represents 50 μm.

(B) Immunofluorescence stainings of TTN3 (red) and insulin (green) in isolated β-cell. Scale bar represents 10 μm.

(C) (Left panel) Representative RT-PCR analysis for gene expression of TTN3 in mouse pancreatic β-cell line, NIT-1, and pancreatic islets of WT and *Ttn3* KO mice. GAPDH (glyceraldehyde-3-phosphate dehydrogenase) was used as a control. PCR products were measured around 450 base pairs. (Right panel) Quantification analysis of *Ttn3* transcript levels relative to housekeeping gene GAPDH in WT and *Ttn3* KO pancreatic islets (n = 3). Data are presented as mean ± SEM. **p < 0.01, Student's t test.

(D and E) Representative traces of mechanically activated inward currents elicited by different membrane displacement steps in primary β-cells from WT (D) and *Ttn3* KO (E) mice.

(F) Summary of the peak amplitude of mechanically activated currents measured in WT (n = 10) and *Ttn3* KO (n = 7) primary β-cells. Data are presented as mean ± SEM. **p < 0.01, Student's t test. The primary β-cells were prepared from five WT and two *Ttn3* KO mice.

mechanisms for the K_{ATP}-channel-independent pathways is swelling-stimulated insulin secretion (Blackard et al., 1975; Drews et al., 1998; Gembal et al., 1992; Takii et al., 2006), as pancreatic β-cells are inflated by high glucose (Miley et al., 1997; Nakayama et al., 2012; Semino et al., 1990). Through exposure to high concentrations of glucose, metabolites, such as lactate, accumulate inside the β-cells, which in sequence increases intracellular osmolality and induces water influx. This glucose-induced swelling of β-cells leads to the stretch of the cell membrane, which consecutively opens stretch-activated cation (SAC) channels. (Nakayama et al., 2012; Takii et al., 2006) Indeed, its channel activity was observed as SAC channel blockers, such as gadolinium, amiloride, 2-APB, and ruthenium red, inhibit the swelling-stimulated insulin secretion in murine pancreatic β-cells (Nakayama et al., 2012; Takii et al., 2006). Some transient receptor potential (TRP) channels, such as TRPV4 and TRPV2, have been proposed as candidate genes for SAC channels. However, there was no direct evidence that these TRP channels mediate the glucose-stimulated insulin secretion by swelling in β-cells (Casas et al., 2008; Hisanaga et al., 2009). Therefore, the molecular identity of the SAC channel responsible for glucose-induced cell swelling in pancreatic β-cells remains unknown.

We identified Tentonin 3/TMEM150C (TTN3) as a cation channel activated by mechanical stimulation with unique slow inactivation kinetics (Hong et al., 2016). Present in dorsal-root ganglion neurons and muscle spindle afferents, TTN3 is known to mediate muscle coordination. In addition, TTN3 is known to mediate blood pressure control as it is expressed in baroreceptors in the aortic arch and actively senses constantly changing blood pressures (Lu et al., 2020). Besides dorsal-root and nodose-ganglion neurons, TTN3 is also expressed highly in the murine pancreas (Hong et al., 2016), proposing a role in pancreatic function. In the present study, we found that TTN3 is highly expressed only in pancreatic β-cells and regulates glucose-stimulated insulin secretion *in vivo*.

RESULTS

TTN3 is expressed in mouse pancreatic β-cells

Previous findings suggest a high mRNA level of *Ttn3* in mouse pancreas (Hong et al., 2016). To further analyze the detailed localization pattern of TTN3 in the pancreas, sections of wild-type (WT) and *Ttn3* knocked out (KO) murine pancreas were stained with TTN3 antibody together with pancreatic cell markers. Surprisingly, WT pancreatic cells that are insulin positive expressed TTN3, whereas an exocrine marker, amylase, or an alpha cell marker, glucagon, failed to colocalize with TTN3 (Figure 1A). *Ttn3* KO pancreatic cells failed to show TTN3 immunofluorescence (Figure 1A). Single β-cells were dissociated from pancreatic islets of WT mice and were identified as β-cells by their large sizes and granular morphologies (Majid et al., 2001). These dissociated cells displayed TTN3 and insulin co-expression (Figure 1B). *Ttn3* mRNA transcripts were also observed in a mouse pancreatic β-cell line, NIT-1 cells, and WT, but not in *Ttn3* KO pancreatic islets (Figure 1C).

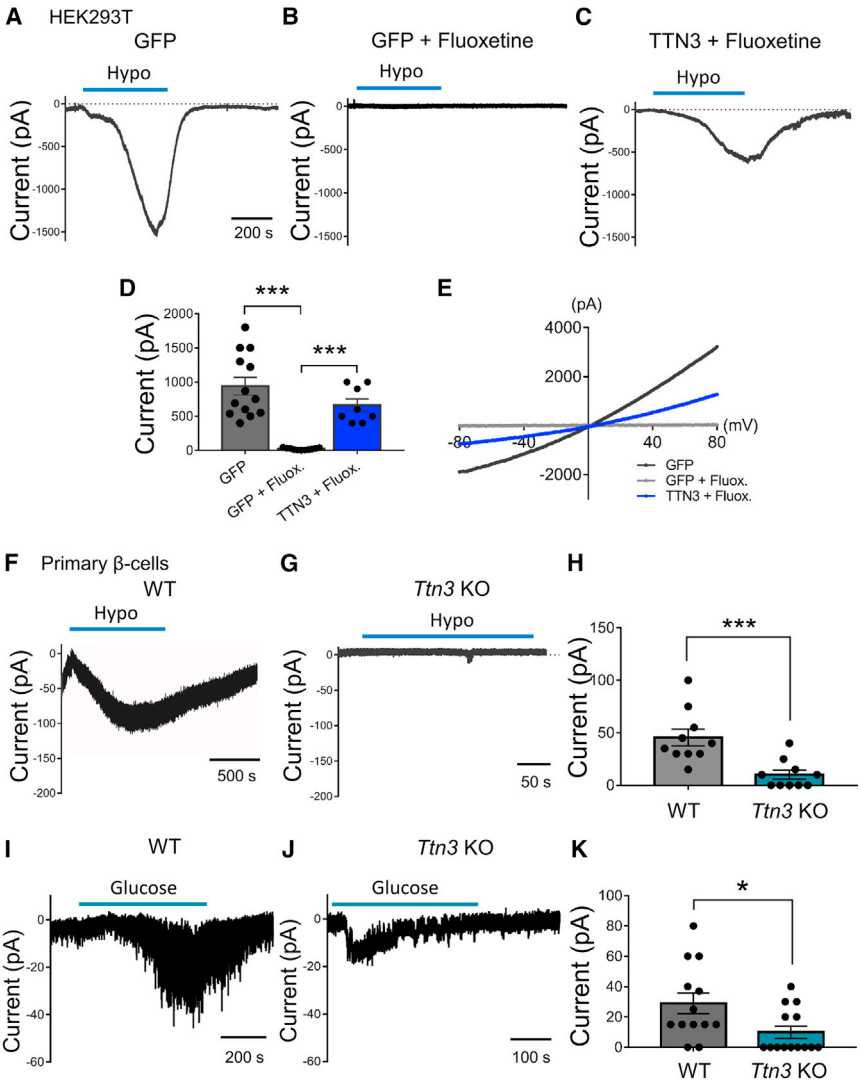

Figure 2. TTN3 is activated by both hypotonicity and glucose

(A and B) Representative traces of hypotonicity (210 mOsm/kg)-induced currents in HEK293T cells transfected with *Gfp* (n = 13) in a control bath solution (A) and in the presence of 100 μM fluoxetine, a volume-regulated anion channel blocker (n = 11) (B). Time scale is identical in (A)–(C). Note a complete block of volume-regulated anion channel current by fluoxetine.

(C) Representative trace of hypotonicity (210 mOsm/kg)-induced current in HEK293T cells transfected with *Ttn3* in the presence of 100 μM fluoxetine (n = 8). Note a robust current evoked by the hypotonicity in the presence of fluoxetine.

(D) Summary of amplitudes of hypotonicity-induced currents in HEK293T cells transfected with *Gfp* or *Ttn3* in the absence or presence of fluoxetine. Data are presented as mean ± SEM. ***p < 0.001, one-way ANOVA with Tukey's post hoc test.

(E) Representative current-voltage (I-V) relationships of hypotonicity-induced currents in HEK293T cells expressing GFP or TTN3 in the absence (dark gray) or presence of fluoxetine (blue).

(F and G) Representative traces of hypotonicity (210 mOsm/kg)-induced currents in primary β-cells from WT (F) and *Ttn3* KO mice (G). In order to block anion currents, both the recording electrode and bath solutions contained sodium gluconate as the main charge carriers.

(H) Summary of hypotonicity-induced current amplitudes in WT (n = 10) and *Ttn3* KO (n = 10) primary β-cells. The primary β-cells were prepared from five WT and five *Ttn3* KO mice. Data are presented as mean ± SEM. ***p < 0.001, Student's t test.

(I and J) Representative traces of high glucose (20 mM)-induced currents in β cells from WT (I) and *Ttn3* KO mice (J). Both the recording electrode and bath solutions contained sodium gluconate as the main charge carriers.

(K) Summary of glucose-induced inward current amplitudes in WT (n = 13) and *Ttn3* KO (n = 14) primary β-cells. The primary β-cells were prepared from five WT and five *Ttn3* KO mice. Data are presented as mean ± SEM. *p < 0.05, Student's t test.

As TTN3 was initially identified as a mechanosensitive cation channel with distinct inactivation kinetics, we investigated if the slowly inactivating currents to mechanical stimuli are observed in isolated β-cells. Indeed, when mechanical steps were applied to the pancreatic β-cells, the slowly inactivating currents, a unique biophysical property of TTN3, were observed (Figures 1D and 1F). However, the mechanically activated currents with the slow inactivation kinetics were not observed in β-cells isolated from *Ttn3* KO mice (Figures 1E and 1F). Collectively, these data indicate the presence of a functional TTN3 channel in pancreatic β-cells.

TTN3 mediates glucose-induced cation currents in pancreatic β-cells

We asked whether TTN3 is activated by glucose- or hypotonicity-induced cell swelling, a well-known mechanical stimulus in β-cells (Nakayama et al., 2012). We first transfected *Gfp* to human embryonic kidney 293T (HEK293T) cells and then stimulated them with a hypotonic (210 mOsm/kg) solution. HEK293T cells are known to express volume-regulating anion channels (VRACs) that evoke large inward currents to hypotonic stimulation (Figures 2A and 2D). These hypotonicity-induced currents were blocked by a chloride channel blocker, fluoxetine (Maertens et al., 1999; Figures 2B and 2D). In HEK293T cells transfected with *Ttn3*, however, the hypotonic solution induced robust inward currents even in the presence of 100 μM fluoxetine (Figures 2C and 2D). The current-voltage relationship was further determined to confirm that the ionic flux observed in *Ttn3*-overexpressed HEK293T cells in the presence of fluoxetine is a cationic current (Figure 2E).

We next explored the functional role of TTN3 in isolated pancreatic β-cells. To exclude the involvement of anionic currents in response to volume change, intracellular Cl^- was replaced with the impermeable anion Na-Gluconate (McLarnon et al., 2000). The application of the hypotonic (210 mOsm/kg) solution robustly evoked inward currents in isolated β-cells of WT

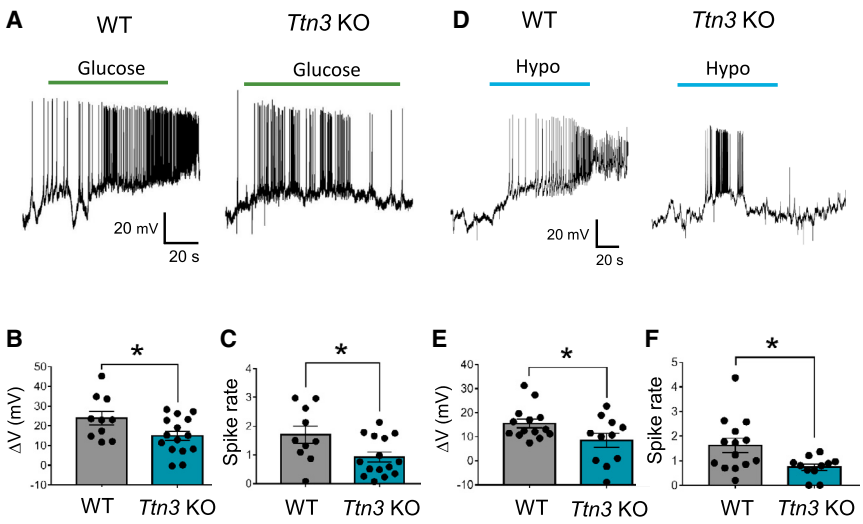

Figure 3. Firing activities of β-cells from *Ttn3* KO mice are reduced in response to glucose and hypotonic stimulations

(A) Representative traces of high glucose (20 mM)-evoked electrical activity in WT (left) and *Ttn3* KO (right) primary β-cells.

(B and C) Summary of glucose-induced membrane depolarization (B) and action potential firing rates (C) in WT (n = 10) and *Ttn3* KO (n = 15) primary β-cells. The primary β-cells were prepared from four WT and six *Ttn3* KO mice. Data are presented as mean ± SEM. *p < 0.05, Student's t test.

(D) Representative traces of hypotonicity (210 mOsm/kg)-evoked electrical activity in WT (left) and *Ttn3* KO (right) primary β-cells.

(E and F) Summary of hypotonicity-induced membrane depolarization (E) and action potential firing rates (F) in WT (n = 14) and *Ttn3* KO (n = 11) primary β-cells. The primary β-cells were prepared from four WT and five *Ttn3* KO mice. Data are presented as mean ± SEM. *p < 0.05, Student's t test.

mice, whereas the currents were markedly reduced in *Ttn3* KO β-cells (Figures 2F–2H). Next, we determined whether glucose-induced swelling is also sufficient to evoke currents through TTN3 in β-cells, as high glucose results in β-cell membrane stretch, due to the osmolality changes derived by the accumulation of metabolites (Blackard et al., 1975; Drews et al., 1998; Miley et al., 1997; Takii et al., 2006). Similar to the hypotonic stimulation, the application of high glucose (20 mM) also evoked inward currents in WT pancreatic β-cells, but the responses were significantly reduced in *Ttn3*-deficient β-cells (Figures 2I–K). These data suggest that TTN3 mediates glucose-induced cation currents in mouse pancreatic β-cells.

TTN3 contributes to the glucose-induced excitation of β-cells

Pancreatic β-cells are excitable cells eliciting action potential firings in response to glucose stimulation (Ashcroft et al., 1984; Ashcroft and Rorsman, 1989; Henquin and Meissner, 1984; Miley et al., 1997). Therefore, we determined if TTN3 contributes to the glucose-induced electrical activities of β-cells. Application of 20 mM glucose to WT isolated β-cells induced a barrage of action potential firings along with depolarization. However, glucose-induced spiking rates and membrane depolarization in *Ttn3* KO β-cells decreased significantly compared to those of WT β-cells (Figures 3A–3C). Similarly, hypotonic (210 mOsm/kg) stimulation of β-cells from both genotypes evoked depolarization with action potential firings (Figures 3D–3F). Notably, β-cells from *Ttn3* KO mice showed significantly reduced firing rates as well as depolarization in comparison with those of WT β-cells. These results suggest that TTN3 is responsible for the electrical activity induced by glucose stimulation in β-cells.

TTN3 evokes Ca^{2+} influx to glucose stimulation

In the process of glucose-stimulated insulin secretion in pancreatic β-cells, intracellular Ca^{2+} concentration is a key determinant of insulin secretion (Kohnert et al., 1979). Therefore, we determined the intracellular Ca^{2+} concentration ($[Ca^{2+}]_i$) of pancreatic β-cells in response to glucose and hypotonic stimulations. Initially, the efficiency of the *Ttn3* small interfering RNA (siRNA) was tested in the NIT-1 cell line. As a result, the downregulation of TTN3 expression was established (Figure 4A). In NIT-1 cells treated with scrambled siRNA, the application of high glucose (20 mM) rapidly elevated $[Ca^{2+}]_i$, whereas cells treated with the *Ttn3* siRNA evoked significantly reduced levels of $[Ca^{2+}]_i$ through glucose stimulation (Figures 4B and 4D). Likewise, the hypotonic solution (210 mOsm/kg) caused a rapid elevation of $[Ca^{2+}]_i$ in scrambled-siRNA-transfected NIT-1 cells, whereas *Ttn3*-siRNA-transfected NIT-1 cells showed a significant decrease in the Ca^{2+} influx (Figures 4C and 4E). Similarly, the effects of a glucose- or hypotonicity-induced increase in $[Ca^{2+}]_i$ were tested on primary cultured β-cells isolated from both genotypes of mice. Both glucose and hypotonic stimulations evoked a sustained increase in $[Ca^{2+}]_i$ in WT β-cells, whereas *Ttn3* KO primary β-cells showed significantly reduced Ca^{2+} responses to these stimulations (Figures 4F–4I). A high KCl (30 mM)-induced increase in $[Ca^{2+}]_i$ demonstrated that the β-cells were electrically viable in both genotypes (Figures 4F and 4G). Together, these data demonstrate that TTN3 regulates glucose- and hypotonicity-induced Ca^{2+} influx in pancreatic β-cells.

The depolarization evoked by the closure of the K_{ATP} channel largely accounts for the increase in glucose-induced $[Ca^{2+}]_i$ (Ashcroft and Rorsman, 1990). Therefore, to exclude K_{ATP}-channel-derived Ca^{2+} influx, we treated an opener of the K_{ATP} channel, diazoxide (Guldstrand et al., 2002). In the presence of 100 μM diazoxide, WT pancreatic β-cells displayed a small but robust elevation of $[Ca^{2+}]_i$ in response to high glucose (20 mM), whereas *Ttn3* KO β-cells showed an elevation in $[Ca^{2+}]_i$ with a reduced degree of increase (Figures 5A and 5C). In addition, even when the VRAC channel was blocked by fluoxetine (100 μM) (Figure 5B), hypotonic stimulation still evoked a rapid and sustained increase in $[Ca^{2+}]_i$ in WT primary β-cells, whereas in *Ttn3* KO primary β-cells, the rise in $[Ca^{2+}]_i$ was significantly diminished (Figures 5B and 5D).

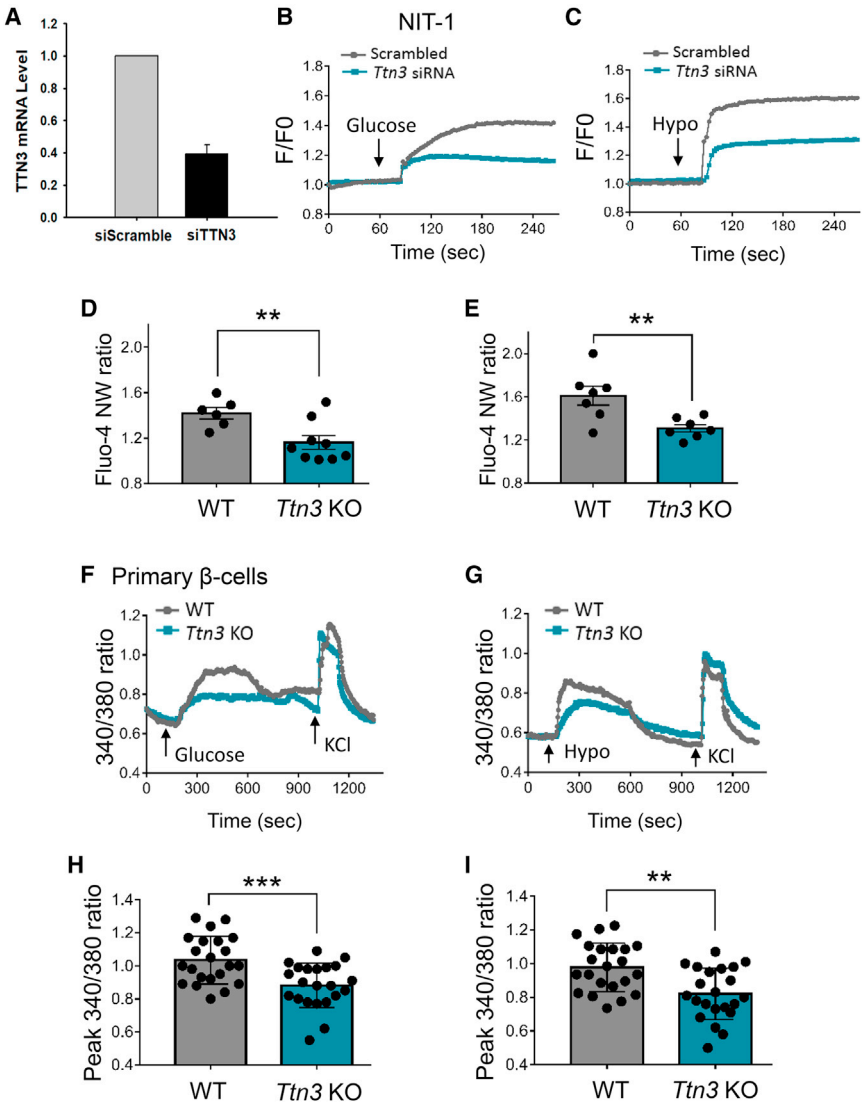

Figure 4. Glucose- and hypotonicity-induced Ca^{2+} influxes are reduced in *Ttn3* KO β-cells

(A) mRNA levels of TTN3 in NIT-1 cell lines treated with either scrambled or *Ttn3* small interfering RNA (siRNA). The experiments were repeated three times (n = 3). Data are presented as mean ± SEM.

(B and C) Average traces of intracellular Ca^{2+} to high glucose (B; 20 mM) and hypotonic (C; 210 mOsm/kg) stimulation in Fluo-4 NW loaded NIT-1 cells transfected with scrambled (gray) or *Ttn3* siRNA (cyan).

(D and E) Mean peak values of Fluo-4 NW fluorescence ratios in WT (gray) and *Ttn3* knockdown NIT-1 cells (cyan) to glucose (D) and hypotonic (E) stimulations. For glucose stimulation, WT (n = 6) and *Ttn3* KO (n = 9); and hypotonic stimulation, WT (n = 7) and *Ttn3* KO (n = 7). Data are presented as mean ± SEM. **p < 0.01, Student's t test.

(F and G) Average traces of intracellular Ca^{2+} of Fura-2-loaded primary β-cells from WT (gray) and *Ttn3* KO mice (cyan) to glucose (F) and hypotonic (G) stimulations. A high KCl (30 mM) solution (arrow) was challenged to confirm cellular excitability.

(H and I) Mean peak values of Fura-2 ratios (340/380 nm) from isolated WT (gray) and *Ttn3* KO (cyan) primary β-cells to glucose (H) and hypotonic (I) stimulation. For glucose stimulation, WT (n = 22) and *Ttn3* KO (n = 22); for hypotonic stimulation, WT n = (22) and *Ttn3* KO (n = 22). Fluorescence intensity was measured every 3 s. The primary β-cells for the glucose test were prepared from four WT and five *Ttn3* KO mice, whereas β-cells for the hypotonic solution test were prepared from five WT and five *Ttn3* KO mice. Data are presented as mean ± SEM. **p < 0.01, ***p < 0.001, Student's t test.

Impaired glucose tolerance and insulin secretion in TTN3-deficient mice

To determine the physiological role of TTN3 in glucose-stimulated insulin secretion, the amount of insulin released upon glucose stimulation was measured in NIT-1 cells, treated with the scrambled siRNA or *Ttn3* siRNA. The application of high glucose (16.7 mM) solution to NIT-1 cells treated with scrambled siRNA induced a 2.5-fold increase in insulin secretion compared to that of low glucose (2.5 mM) application. In contrast, the administration of a high glucose solution to NIT-1 cells transfected with *Ttn3* siRNA induced a 1.6-fold increase in insulin secretion compared to that of the low glucose application to these cells (Figure 6A).

Next, we further expanded glucose-stimulated insulin secretion measurements on littermate WT and *Ttn3* KO pancreatic islets. Three different glucose concentrations, namely, 2.5, 5.0, and 20 mM, were applied to the islets of both genotypes. The amount of insulin secretion load was indistinct between littermate WT and *Ttn3* KO islets after low glucose (2.5 mM) stimulation. At the basal level of glucose (5.0 mM), islets from both genotypes of mice showed an increase in insulin secretion. However, *Ttn3* KO mice produced less insulin at the glucose challenge than littermate WT mice. Stimulation of high glucose (20 mM) to both littermate WT and *Ttn3* KO islets led to a significant increase in insulin levels, whereas *Ttn3* KO islets excreted lesser amounts of insulin than littermate WT islets (Figure 6B). The islet morphology of both genotypes appeared grossly similar and normal (Figures S1A and S1B), indicating that the β-cell itself is intact from the loss of *Ttn3*. Beta-cell masses and insulin contents were also indistinguishable between both genotypes (Figures 6C and 6D).

Next, we assessed the effects of *Ttn3* ablation on the ability to metabolize glucose in littermate WT and *Ttn3* KO mice. An intraperitoneal (i.p.) glucose tolerance test was conducted in littermate WT and *Ttn3* KO mice that were fasted overnight (16 h). The i.p. injection of glucose (2 g/kg body weight) elevated the blood glucose level in both genotypes (Figure 6E), whereas the basal blood glucose levels of both genotypes were similar. However, *Ttn3* KO mice showed a significant

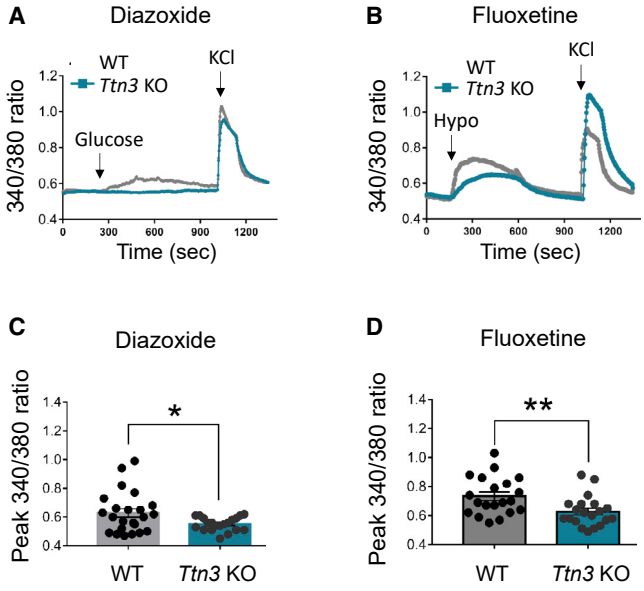

Figure 5. TTN3-mediated Ca^{2+} influx is independent of K_{ATP} or volume-regulated anion channel activity

(A) High glucose (20 mM)-induced intracellular Ca^{2+} of Fura-2 loaded primary β-cells from WT and *Ttn3* KO mice in the presence of K_{ATP} channel opener diazoxide (100 μM).

(B) Hypotonicity (210 mOsm/kg)-induced intracellular Ca^{2+} in Fura-2-loaded primary β-cells from WT and *Ttn3* KO mice in the presence of volume-regulated anion channel blocker fluoxetine (100 μM).

(C and D) Mean peak values of Ca^{2+} transients of primary β-cells from WT and *Ttn3* KO mice in the presence of diazoxide (C) and fluoxetine (D). For diazoxide treatment, WT (n = 23) and *Ttn3* KO (n = 20); for fluoxetine treatment, WT (n = 20) and *Ttn3* KO (n = 20). The primary β-cells for diazoxide application were prepared from five WT and five *Ttn3* KO mice, whereas primary β-cells for fluoxetine application were prepared from four WT and five *Ttn3* KO mice. Data are presented as mean ± SEM. *p < 0.05; **p < 0.01, Student's t test.

increase in the blood glucose level at 15 and 30 min after the injection (Figure 6E). Because the ablation of *Ttn3* leads to the impaired glucose tolerance, we questioned whether the impaired glucose tolerance is due to decreased insulin sensitivity. Thus, we conducted an i.p. insulin tolerance test, for which the blood glucose levels at different time points were measured after injection of Humulin R (0.5 U/kg) in fasted (6 h) mice. As a result, blood glucose levels from both genotypes at 2 h after the i.p. Humulin R injection were identical, indicating that the loss of *Ttn3* does not alter insulin sensitivity (Figure 6F).

We determined the effects of TTN3 on glucose-stimulated insulin release *in vivo*. Serum insulin levels every 10 min for 30 min after injection of glucose (2 g/kg body weight) in fasted (16 h) mice were measured. The serum insulin level was elevated in both genotypes 10 min after the glucose stimulation. However, the serum insulin level in *Ttn3*-deficient mice was significantly lower than that of littermate WT mice (Figure 6G). Interestingly, at 0 min, the serum insulin levels of Ttn3 KO mice were lower than those of littermate WT mice. These results suggest that the genetic ablation of *Ttn3* leads to impaired glucose tolerance due to the decreased insulin secretion.

DISCUSSION

Glucose homeostasis is tightly regulated by the pancreatic endocrine hormones insulin and glucagon, which lowers and raises blood sugar, respectively. Diabetes mellitus is a metabolic disease characterized by a blood glucose level that is not maintained within a controlled range due to impaired insulin sensitivity or insufficient insulin secretion from pancreatic β-cells (Ashcroft and Rorsman, 2012; Porte and Kahn, 2001). Moreover, it is followed by severe complications such as retinopathy, neuropathy, nephropathy, and atherosclerosis (Zheng et al., 2018). Molecular mechanisms underlying the glucose-stimulated insulin secretion in pancreatic β-cells have been studied intensely. The involvement of the K_{ATP} channel in insulin secretion becomes the leading pathway for glucose-stimulated insulin secretion. However, alternative pathways for glucose-stimulated insulin secretion are also suggested (Blackard et al., 1975; Drews et al., 1998; Gembal et al., 1992; Takii et al., 2006). Stretch-activated channel activity is suggested as one of the alternative mechanisms for glucose-stimulated insulin secretion (Nakayama et al., 2012; Takii et al., 2006). The molecular identity of the SAC channel, however, remained unknown. In the present study, we suggest for the following reasons that TTN3 is an additional regulator for glucose-stimulated insulin secretion in pancreatic β-cells (Figure 7): (1) it has selective expression in β-cells, (2) TTN3-like mechanosensitive currents occur in pancreatic β−cells, (3) genetic ablation of *Ttn3* in pancreatic β-cells leads to decreased calcium influx and electrical activity in response to glucose stimulation, and (4) *Ttn3* gene deletion leads to impaired glucose tolerance with decreased insulin secretion *in vivo*. More importantly, TTN3 appears to be active in regulating the insulin secretion even at the basal level of glucose because the serum insulin level was significantly lower in *Ttn3* KO mice (Figure 6G). The reduced insulin secretion from *Ttn3* KO islets in response to 5.0 mM glucose may account for the reduced serum insulin in *Ttn3* KO mice at the basal level of glucose (Figure 6B).

Glucose-stimulated insulin secretion is regulated by the cytoplasmic concentration of Ca^{2+}, which mediates membrane docking, tethering, and exocytosis of insulin granules. Several studies unveiled the mechanism of Ca^{2+} signaling in pancreatic β-cells upon glucose stimulation (Rorsman and Ashcroft, 2018; Wollheim and Sharp, 1981). The source of intracellular Ca^{2+} increase is the extracellular Ca^{2+} through voltage-gated Ca^{2+} channels, which are activated by β-cell depolarization (Hiriart et al., 2014; Yang and Berggren, 2005). The major component responsible for the β-cell depolarization is thought to be the closure of K_{ATP} channels (Henquin, 2009; Seghers et al., 2000). However, several studies suggest that the K_{ATP} channel is not the sole ionic mechanism underlying the depolarization and predict the presence of additional contributors for the depolarization of β-cells (Best, 2002; Best et al., 1992b; Blackard et al., 1975) In line with this notion, swelling of the β-cells induced by glucose is also considered a significant factor stimulating insulin secretion (Blackard et al., 1975; Miley et al., 1997; Takii et al., 2006) Exposed to a high concentration of glucose, β-cells accelerate the process of glycolysis, which leads to an intracellular lactate accumulation (Best et al., 1992a; Davies et al., 2007; Miley et al., 1997). The accumulation of lactate results in intracellular hyper-osmolality

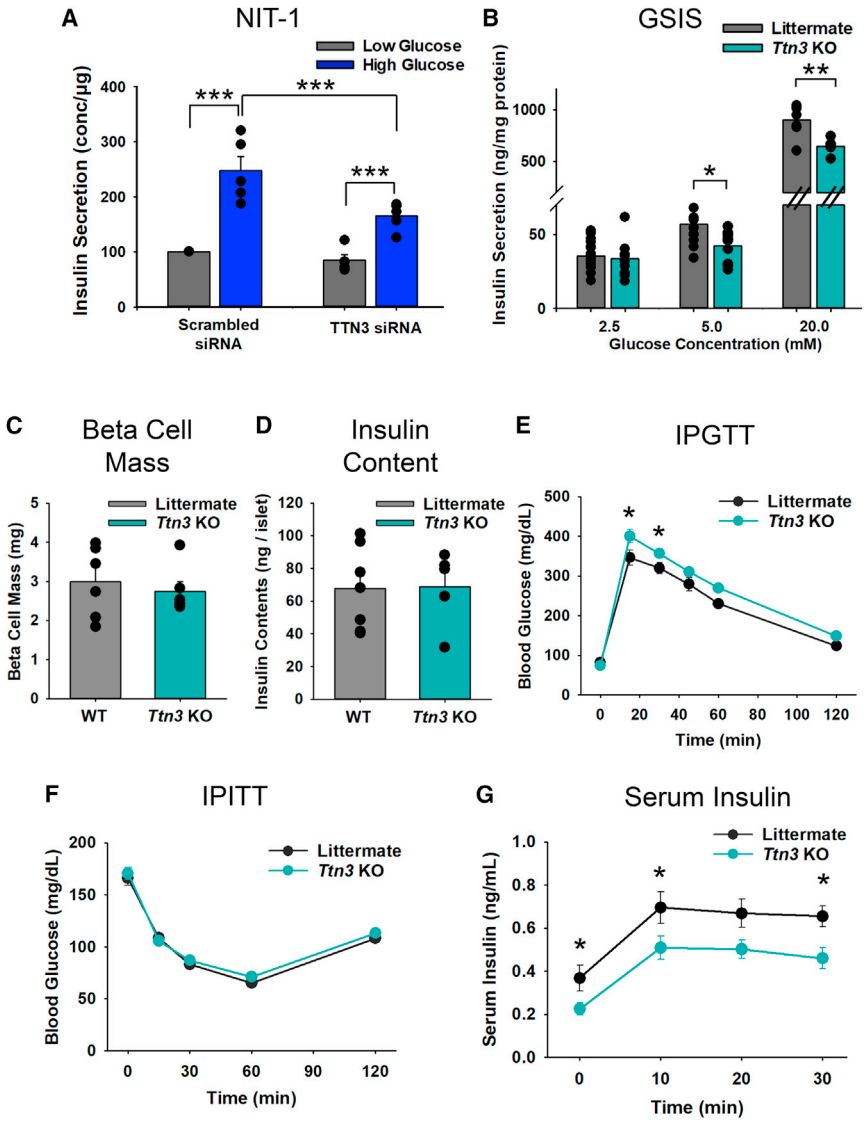

Figure 6. The genetic ablation of *Ttn3* impairs glucose-stimulated insulin secretion *in vivo*

(A) Glucose-stimulated insulin secretion of NIT-1 cells treated with *Ttn3* siRNA (n = 5) or scrambled siRNA (n = 5) to low glucose (2.5 mM) and high glucose (20 mM). Data are presented as mean ± SEM. ***p < 0.001, Student's t test.

(B) Glucose-stimulated insulin secretion of littermate WT and *Ttn3* KO pancreatic islets stimulated with 2.5, 5.0, or 20.0 mM glucose concentrations. The pancreatic islets were prepared from 13 littermate WT and 10 *Ttn3* KO mice. Data are presented as mean ± SEM. *p < 0.05; **p < 0.01, Student's t test.

(C) The β-bell mass of littermate WT and *Ttn3* KO pancreas. Pancreases were extracted from six littermate WT and six *Ttn3* KO mice. Data are presented as mean ± SEM.

(D) Insulin contents of pancreatic islets from littermate WT and *Ttn3* KO mice after glucose-stimulated insulin secretion. Insulin contents were normalized from total protein mass. Pancreatic islets were prepared from seven littermate WT and five *Ttn3* KO mice. Data are presented as mean ± SEM.

(E and F) Intraperitoneal glucose tolerance tests (IPGTTs) (E) and intraperitoneal insulin tolerance tests (IPITTs) (F). The levels of glucose in blood were measured in littermate WT (n = 8) and *Ttn3* KO (n = 8) mice at every 15 or 30 min after 16 h of fasting. Glucose (2 g/kg body weight) (E) or Humulin R (0.5 U/kg body weight) (F) in saline was administered at time zero. Data are presented as mean ± SEM. *p < 0.05, Student's t test.

(G) The levels of insulin in serum were measured in littermate WT (n = 8) and *Ttn3* KO (n = 9) mice at every 10 min after the administration of glucose (2 g/kg body weight). Data are presented as mean ± SEM. *p < 0.05, Student's t test.

that draws water by aquaporin 7 into the cell (Louchami et al., 2012; Sekine et al., 1994). Even in the absence of glucose, osmotic swelling of β-cells induced insulin secretion (Best et al., 1996; Blackard et al., 1975; Drews et al., 1998). Thus, swelling itself is one of the triggering pathways to insulin secretion.

The role of VRAC in β-cells has been studied (Miley et al., 1997; Nakayama et al., 2012; Semino et al., 1990). VRAC can depolarize β-cells because they mediate the efflux of anion Cl^-. In fact, the equilibrium potential of Cl^- is relatively high (−30 mV) in β-cells, which leads to the depolarization of the cell (Drews et al., 1998; Kinard and Satin, 1995). The molecular identity of the VRAC was identified to be SWELL1/LRRC8A (Qiu et al., 2014). Recently, it has been shown that SWELL1 has an important role in glucose sensing and therefore enhancing insulin secretion as SWELL1-deficient mice showed impaired glucose tolerance and insulin secretion (Kang et al., 2018; Stuhlmann et al., 2018).

The presence of SAC channels along with the VRAC in pancreatic β-cells has also been suggested as their blockers, such as gadolinium, amiloride, 2-APB, and ruthenium red, inhibit the swelling-stimulated insulin secretion in β-cells (Nakayama et al., 2012; Takii et al., 2006). In addition, the treatment of anion channel blockers to β-cells partially blocked the swelling-induced Ca^{2+} influx or insulin secretion (Kinard et al., 2001). The present study showed that mechanical step stimuli evoked currents with slow inactivation kinetics that are absent in β-cells of *Ttn3* KO mice and *Ttn3*-overexpressing cells responded to hypotonic stimulation. In addition, cationic currents and intracellular Ca^{2+} increase evoked by a hypotonic solution were markedly reduced in *Ttn3*-deficient β-cells. Thus, these data suggest that TTN3 may be a key component of SAC channels in β-cells, which sense mechanical tension of the plasma membrane and transduce it to electrical activity in β-cells.

TTN3 has been recently determined as a mechanosensitive non-selective cation channel (Hong et al., 2016). TTN3 is activated by mechanical step stimuli but inactivates slowly, which

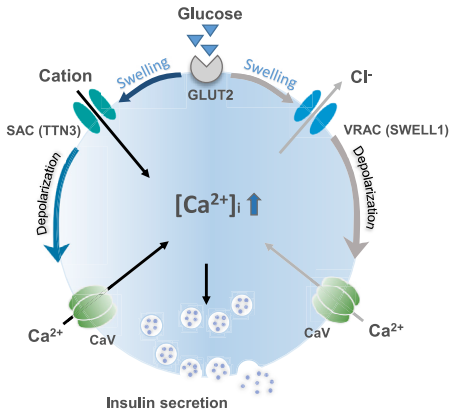

Figure 7. A mechanism of swelling-induced insulin secretion in β-cells by TTN3

SAC, stretch-activated cation channel; VRAC, volume-regulated anion channel.

is in good contrast with rapidly inactivating Piezo channels. However, because TTN3 mechanosensitivity is lost in *Piezo1*-deficient HEK cells, the role of TTN3 as a mechanosensor was questioned (Anderson et al., 2018; Dubin et al., 2017; Hong et al., 2017). Instead, TTN3 is suggested to be a modulator of Piezo1. However, we found that TTN3 evokes robust mechanically activated currents in the *Piezo1*-deficient HEK cells when these cells are treated with jasplakinolide, an actin polymerizing agent, suggesting that TTN3 mechanosensitivity is independent of Piezo1 (Bubb et al., 1994; Lu et al., 2020).

Piezo1 is expressed in acinar cells and is involved in pressure-induced pancreatitis (Romac et al., 2018; Swain et al., 2020). Thus, Piezo1 and TTN3 appear to play different roles in the pancreas. However, recently, Piezo1 has been reported to be involved in insulin release in islets (Deivasikamani et al., 2019). Piezo1 transcripts are present in β-cell lines, such as INS-1 cells as well as rat islet cells. Yoda1, an agonist of Piezo1, increases intracellular Ca^{2+} and insulin release in the β-cell lines and rat pancreatic islets (Deivasikamani et al., 2019). However, an immunohistochemical analysis reveals that Piezo1 is expressed rarely in insulin-secreting β-cells but expressed in glucagon-secreting α-cells and in amylase-positive cells (Figure S2). Additionally, the knockdown of *Piezo*1 in INS-1 cells fails to reduce the high-glucose-induced insulin release (Deivasikamani et al., 2019). Thus, the involvement of Piezo1 in β-cell function needs to be clarified further.

In summary, TTN3 is expressed in pancreatic beta cells, where it contributes actively to glucose-induced insulin secretion as a stretch-activated channel. Due to this correlation, targeting TTN3 may be useful in the clinic for treating diabetes mellitus.

Limitations of the study

Islets of Langerhans consist of about 80% β-cells, and the remaining cells may be other cell types such as α-cells. In the present study, we did not specifically select β-cells for electrophysiological recordings. Therefore, some of the recordings might be made on other cell types.

In addition, for *in vivo* experiments, *Ttn3* whole KO mice were used. Thus, the *in vivo* results could have been influenced by the ablation of *Ttn3* in other regions. TTN3 is lacking in the CNS, suggesting the effect of *Ttn3* ablation in the CNS may be minimal. TTN3 is also known to sense blood pressure changes in baroreceptors (Lu et al., 2020). Thus, *Ttn3* KO mice have higher blood pressure. However, this change in blood pressure control is limited only to the peripheral baroreceptor function, as the central control system of the KO mice is not affected by the genetic deletion of *Ttn3* (Lu et al., 2020). This could imply that other off-target effects of the whole *Ttn3* KO may be minimal to insulin release in beta cells.

STAR★METHODS

Detailed methods are provided in the online version of this paper and include the following:

- KEY RESOURCES TABLE
- RESOURCE AVAILABILITY
  - Lead contact
  - Materials availability
  - Data and code availability
- EXPERIMENTAL MODEL AND SUBJECT DETAILS
  - Animals
  - Cell Line Culture and Transfection
  - Primary culture of pancreatic β-cells
- METHOD DETAILS
  - Immunohistochemistry
  - RT-PCR
  - Calcium Measurements
  - Electrophysiology
  - Solutions
  - Mechanical Stimulation
  - Insulin Assay
  - β-cell mass measurement
- QUANTIFICATION AND STATISTICAL ANALYSIS
  - Transcript Level Quantification
  - Statistical Analysis

SUPPLEMENTAL INFORMATION

Supplemental information can be found online at https://doi.org/10.1016/j.celrep.2021.110067.

ACKNOWLEDGMENTS

We thank Prof. Greg Suh for his constructive feedback. This study was supported by the National Research Foundation of Korea (2020R1A3A300192911) and the KIST Institutional Program (project no. 1711124215).

AUTHOR CONTRIBUTIONS

J.W. designed the research, conducted experiments, and analyzed data. J.N. assisted with the immunohistochemistry study. G.-S.H., T.K., S.P., and H.K. performed electrophysiology studies. J.S.L. performed the *in vitro* insulin assay. S.P. assisted with *in vivo* experiments. K.S.P. and U.O. directed research and wrote the manuscript.

DECLARATION OF INTERESTS

U.O. and J.W. have a registered patent in the Republic of Korea for the use of Tentonin 3 for developing treatments of diabetes mellitus (KR-10-2019-0083428).

Received: August 19, 2020
Revised: October 17, 2021
Accepted: November 8, 2021
Published: November 30, 2021

REFERENCES

Anderson, E.O., Schneider, E.R., Matson, J.D., Gracheva, E.O., and Bagriantsev, S.N. (2018). TMEM150C/Tentonin3 Is a Regulator of Mechano-gated Ion Channels. Cell Rep. *23*, 701–708.

Ashcroft, F.M., and Rorsman, P. (1989). Electrophysiology of the pancreatic beta-cell. Prog. Biophys. Mol. Biol. *54*, 87–143.

Ashcroft, F.M., and Rorsman, P. (1990). ATP-sensitive K+ channels: a link between B-cell metabolism and insulin secretion. Biochem. Soc. Trans. *18*, 109–111.

Ashcroft, F.M., and Rorsman, P. (2012). Diabetes mellitus and the β cell: the last ten years. Cell *148*, 1160–1171.

Ashcroft, F.M., Harrison, D.E., and Ashcroft, S.J. (1984). Glucose induces closure of single potassium channels in isolated rat pancreatic beta-cells. Nature *312*, 446–448.

Best, L. (2002). Evidence that glucose-induced electrical activity in rat pancreatic beta-cells does not require KATP channel inhibition. J. Membr. Biol. *185*, 193–200.

Best, L., Trebilcock, R., and Tomlinson, S. (1992a). Lactate transport in insulin-secreting beta-cells: contrast between rat islets and HIT-T15 insulinoma cells. Mol. Cell. Endocrinol. *86*, 49–56.

Best, L., Yates, A.P., and Tomlinson, S. (1992b). Stimulation of insulin secretion by glucose in the absence of diminished potassium (86Rb+) permeability. Biochem. Pharmacol. *43*, 2483–2485.

Best, L., Miley, H.E., and Yates, A.P. (1996). Activation of an anion conductance and beta-cell depolarization during hypotonically induced insulin release. Exp. Physiol. *81*, 927–933.

Blackard, W.G., Kikuchi, M., Rabinovitch, A., and Renold, A.E. (1975). An effect of hyposmolarity on insulin release in vitro. Am. J. Physiol. *228*, 706–713.

Bubb, M.R., Senderowicz, A.M., Sausville, E.A., Duncan, K.L., and Korn, E.D. (1994). Jasplakinolide, a cytotoxic natural product, induces actin polymerization and competitively inhibits the binding of phalloidin to F-actin. J. Biol. Chem. *269*, 14869–14871.

Casas, S., Novials, A., Reimann, F., Gomis, R., and Gribble, F.M. (2008). Calcium elevation in mouse pancreatic beta cells evoked by extracellular human islet amyloid polypeptide involves activation of the mechanosensitive ion channel TRPV4. Diabetologia *51*, 2252–2262.

Cook, D.L., and Hales, C.N. (1984). Intracellular ATP directly blocks K+ channels in pancreatic B-cells. Nature *311*, 271–273.

Davies, S.L., Brown, P.D., and Best, L. (2007). Glucose-induced swelling in rat pancreatic alpha-cells. Mol. Cell. Endocrinol. *264*, 61–67.

Deivasikamani, V., Dhayalan, S., Abudushalamu, Y., Mughal, R., Visnagri, A., Cuthbertson, K., Scragg, J.L., Munsey, T.S., Viswambharan, H., Muraki, K., et al. (2019). Piezo1 channel activation mimics high glucose as a stimulator of insulin release. Sci. Rep. *9*, 16876.

Drews, G., Zempel, G., Krippeit-Drews, P., Britsch, S., Busch, G.L., Kaba, N.K., and Lang, F. (1998). Ion channels involved in insulin release are activated by osmotic swelling of pancreatic B-cells. Biochim. Biophys. Acta *1370*, 8–16.

Dubin, A.E., Murthy, S., Lewis, A.H., Brosse, L., Cahalan, S.M., Grandl, J., Coste, B., and Patapoutian, A. (2017). Endogenous Piezo1 Can Confound Mechanically Activated Channel Identification and Characterization. Neuron *94*, 266–270.e3.

Gembal, M., Gilon, P., and Henquin, J.C. (1992). Evidence that glucose can control insulin release independently from its action on ATP-sensitive K+ channels in mouse B cells. J. Clin. Invest. *89*, 1288–1295.

Guldstrand, M., Grill, V., Björklund, A., Lins, P.E., and Adamson, U. (2002). Improved beta cell function after short-term treatment with diazoxide in obese subjects with type 2 diabetes. Diabetes Metab. *28*, 448–456.

Henquin, J.C. (2009). Regulation of insulin secretion: a matter of phase control and amplitude modulation. Diabetologia *52*, 739–751.

Henquin, J.C. (2011). The dual control of insulin secretion by glucose involves triggering and amplifying pathways in β-cells. Diabetes Res. Clin. Pract. *93*, S27–S31.

Henquin, J.C., and Meissner, H.P. (1984). Significance of ionic fluxes and changes in membrane potential for stimulus-secretion coupling in pancreatic B-cells. Experientia *40*, 1043–1052.

Hiriart, M., Velasco, M., Larqué, C., and Diaz-Garcia, C.M. (2014). Metabolic syndrome and ionic channels in pancreatic beta cells. Vitam. Horm. *95*, 87–114.

Hisanaga, E., Nagasawa, M., Ueki, K., Kulkarni, R.N., Mori, M., and Kojima, I. (2009). Regulation of calcium-permeable TRPV2 channel by insulin in pancreatic beta-cells. Diabetes *58*, 174–184.

Hong, G.S., Lee, B., Wee, J., Chun, H., Kim, H., Jung, J., Cha, J.Y., Riew, T.R., Kim, G.H., Kim, I.B., and Oh, U. (2016). Tentonin 3/TMEM150c Confers Distinct Mechanosensitive Currents in Dorsal-Root Ganglion Neurons with Proprioceptive Function. Neuron *91*, 708–710.

Hong, G.S., Lee, B., and Oh, U. (2017). Evidence for Mechanosensitive Channel Activity of Tentonin 3/TMEM150C. Neuron *94*, 271–273.e2.

Kahn, S.E. (2000). The importance of the beta-cell in the pathogenesis of type 2 diabetes mellitus. Am. J. Med. *108*, 2S–8S.

Kang, C., Xie, L., Gunasekar, S.K., Mishra, A., Zhang, Y., Pai, S., Gao, Y., Kumar, A., Norris, A.W., Stephens, S.B., and Sah, R. (2018). SWELL1 is a glucose sensor regulating β-cell excitability and systemic glycaemia. Nat. Commun. *9*, 367.

Kim, S., Yun, H.M., Baik, J.H., Chung, K.C., Nah, S.Y., and Rhim, H. (2007). Functional interaction of neuronal Cav1.3 L-type calcium channel with ryanodine receptor type 2 in the rat hippocampus. J. Biol. Chem. *282*, 32877–32889.

Kinard, T.A., and Satin, L.S. (1995). An ATP-sensitive Cl- channel current that is activated by cell swelling, cAMP, and glyburide in insulin-secreting cells. Diabetes *44*, 1461–1466.

Kinard, T.A., Goforth, P.B., Tao, Q., Abood, M.E., Teague, J., and Satin, L.S. (2001). Chloride channels regulate HIT cell volume but cannot fully account for swelling-induced insulin secretion. Diabetes *50*, 992–1003.

Kohnert, K.D., Hahn, H.J., Gylfe, E., Borg, H., and Hellman, B. (1979). Calcium and pancreatic beta-cell function. 6. Glucose and intracellular 45Ca distribution. Mol. Cell. Endocrinol. *16*, 205–220.

LeRoith, D. (2002). Beta-cell dysfunction and insulin resistance in type 2 diabetes: role of metabolic and genetic abnormalities. Am. J. Med. *113*, 3S–11S.

Louchami, K., Best, L., Brown, P., Virreira, M., Hupkens, E., Perret, J., Devuyst, O., Uchida, S., Delporte, C., Malaisse, W.J., et al. (2012). A new role for aquaporin 7 in insulin secretion. Cell. Physiol. Biochem. *29*, 65–74.

Lu, H.J., Nguyen, T.L., Hong, G.S., Pak, S., Kim, H., Kim, H., Kim, D.Y., Kim, S.Y., Shen, Y., Ryu, P.D., et al. (2020). Tentonin 3/TMEM150C senses blood pressure changes in the aortic arch. J. Clin. Invest. *130*, 3671–3683.

MacDonald, P.E., Joseph, J.W., and Rorsman, P. (2005). Glucose-sensing mechanisms in pancreatic beta-cells. Philos. Trans. R. Soc. Lond. B Biol. Sci. *360*, 2211–2225.

Maertens, C., Wei, L., Voets, T., Droogmans, G., and Nilius, B. (1999). Block by fluoxetine of volume-regulated anion channels. Br. J. Pharmacol. *126*, 508–514.

Majid, A., Speake, T., Best, L., and Brown, P.D. (2001). Expression of the Na+K+-2Cl- cotransporter in alpha and beta cells isolated from the rat pancreas. Pflugers Arch. *442*, 570–576.

Mathers, C.D., and Loncar, D. (2006). Projections of global mortality and burden of disease from 2002 to 2030. PLoS Med. *3*, e442.

McLarnon, J.G., Helm, J., Goghari, V., Franciosi, S., Choi, H.B., Nagai, A., and Kim, S.U. (2000). Anion channels modulate store-operated calcium influx in human microglia. Cell Calcium *28*, 261–268.

Miley, H.E., Sheader, E.A., Brown, P.D., and Best, L. (1997). Glucose-induced swelling in rat pancreatic beta-cells. J. Physiol. *504*, 191–198.

Nakayama, K., Tanabe, Y., Obara, K., and Ishikawa, T. (2012). Mechanosensitivity of Pancreatic β-cells, Adipocytes, and Skeletal Muscle Cells: The Therapeutic Targets of Metabolic Syndrome. In Mechanically Gated Channels and their Regulation, A. Kamkin and I. Lozinsky, eds. (Springer Netherlands), pp. 379–404.

Porte, D., Jr., and Kahn, S.E. (2001). beta-cell dysfunction and failure in type 2 diabetes: potential mechanisms. Diabetes *50*, S160–S163.

Qiu, Z., Dubin, A.E., Mathur, J., Tu, B., Reddy, K., Miraglia, L.J., Reinhardt, J., Orth, A.P., and Patapoutian, A. (2014). SWELL1, a plasma membrane protein, is an essential component of volume-regulated anion channel. Cell *157*, 447–458.

Ravier, M.A., Nenquin, M., Miki, T., Seino, S., and Henquin, J.C. (2009). Glucose controls cytosolic Ca2+ and insulin secretion in mouse islets lacking adenosine triphosphate-sensitive K+ channels owing to a knockout of the pore-forming subunit Kir6.2. Endocrinology *150*, 33–45.

Romac, J.M., Shahid, R.A., Swain, S.M., Vigna, S.R., and Liddle, R.A. (2018). Piezo1 is a mechanically activated ion channel and mediates pressure induced pancreatitis. Nat. Commun. *9*, 1715.

Rorsman, P., and Ashcroft, F.M. (2018). Pancreatic β-Cell Electrical Activity and Insulin Secretion: Of Mice and Men. Physiol. Rev. *98*, 117–214.

Seghers, V., Nakazaki, M., DeMayo, F., Aguilar-Bryan, L., and Bryan, J. (2000). Sur1 knockout mice. A model for K(ATP) channel-independent regulation of insulin secretion. J. Biol. Chem. *275*, 9270–9277.

Sekine, N., Cirulli, V., Regazzi, R., Brown, L.J., Gine, E., Tamarit-Rodriguez, J., Girotti, M., Marie, S., MacDonald, M.J., Wollheim, C.B., et al. (1994). Low lactate dehydrogenase and high mitochondrial glycerol phosphate dehydrogenase in pancreatic beta-cells. Potential role in nutrient sensing. J. Biol. Chem. *269*, 4895–4902.

Semino, M.C., Gagliardino, A.M., Bianchi, C., Rebolledo, O.R., and Gagliardino, J.J. (1990). Early changes in the rat pancreatic B cell size induced by glucose. Acta Anat. (Basel) *138*, 293–296.

Stuhlmann, T., Planells-Cases, R., and Jentsch, T.J. (2018). LRRC8/VRAC anion channels enhance β-cell glucose sensing and insulin secretion. Nat. Commun. *9*, 1974.

Swain, S.M., Romac, J.M., Shahid, R.A., Pandol, S.J., Liedtke, W., Vigna, S.R., and Liddle, R.A. (2020). TRPV4 channel opening mediates pressure-induced pancreatitis initiated by Piezo1 activation. J. Clin. Invest. *130*, 2527–2541.

Takii, M., Ishikawa, T., Tsuda, H., Kanatani, K., Sunouchi, T., Kaneko, Y., and Nakayama, K. (2006). Involvement of stretch-activated cation channels in hypotonically induced insulin secretion in rat pancreatic beta-cells. Am. J. Physiol. Cell Physiol. *291*, C1405–C1411.

Wollheim, C.B., and Sharp, G.W. (1981). Regulation of insulin release by calcium. Physiol. Rev. *61*, 914–973.

Yang, S.N., and Berggren, P.O. (2005). CaV2.3 channel and PKClambda: new players in insulin secretion. J. Clin. Invest. *115*, 16–20.

Zheng, Y., Ley, S.H., and Hu, F.B. (2018). Global aetiology and epidemiology of type 2 diabetes mellitus and its complications. Nat. Rev. Endocrinol. *14*, 88–98.

Zhuo, X., Zhang, P., and Hoerger, T.J. (2013). Lifetime direct medical costs of treating type 2 diabetes and diabetic complications. Am. J. Prev. Med. *45*, 253–261.

STAR★METHODS

KEY RESOURCES TABLE

REAGENT or RESOURCE	SOURCE	IDENTIFIER
Antibodies		
Anti-Amylase Antibody	Santa Cruz Biotechnology	Cat# SC-46657; RRID: AB_626668
Anti-Glucagon Antibody	Sigma-Aldrich	Cat# G2654; RRID: AB_259852
Anti-Insulin Antibody	Santa Cruz Biotechnology	Cat# SC-8033; RRID: AB_627285
Anti-Mouse Piezo1 Antibody	Novus Biologicals	Cat# NBP1-78537; RRID: AB_11003149
Anti-Tentonin3 Antibody	Hong et al., 2016	N/A
Chemicals, peptides, and recombinant proteins		
D-Glucose	Sigma Aldrich	Cat# G8769; CAS: 50-99-7
Hank's Balanced Salt Solution Medium (with Calcium)	Biowest	Cat# L0612
Dulbecco's Modified Eagle Medium	GIBCO	Cat# 11995
Hank's Balanced Salt Solution Medium (without Calcium)	GIBCO	Cat# 14175
Roswell Park Memorial Institute 1640 Medium	GIBCO	Cat# 11875
Fetal Bovine Serum	GIBCO	Cat# 26140
Penicillin/Streptomycin	GIBCO	Cat# 15140
FuGene® HD	Promega	Cat# E2311
Lipofectamine 3000	Life Technologies	Cat# L3000015
RNAiMax	Invitrogen	Cat# 13778-030
Fluo-4 NW	Invitrogen	Cat# F36206
Fura-2-AM	Molecular Probes	Cat# F1221
Alexa Flour 488	Life Technology	Cat# A21202
Alexa Flour 594	Life Technology	Cat# A10072
Hoechst 33342	Thermo Fisher Scientific	Cat# H3570
DreamTaq Green Polymerase	Thermo Fisher Scientific	Cat # EP0712
Biocoll Gradient	Biochrom	Cat# L6155
Collagenase P	Roche	Cat# 11213865001
Humulin R	Lilly	Cat# HI0210
Zoletil 50 and Rumpon	Virbac	N/A
Critical commercial assays		
Easy-spin Total RNA Extraction Kit	Intron	Cat # 17221
SuperScript III	Invitrogen	Cat # 18080
Mouse Insulin ELISA	ALPCO	Cat # 80-INSMS-E01
Ultra Sensitive Mouse Insulin ELISA Kit	Crystal Chem	Cat # 90080; RRID: AB_2783626
Experimental models: Organisms/strains		
Mouse, C57BL/6J: TTN3/TMEM150C Knockout	Hong et al., 2016	N/A
Experimental models: Cell lines		
HEK293T	ATCC	Cat# CRL-3216; RRID: CVCL_0063
NIT-1	ATCC	Cat# CRL-2055; RRID: CVCL_3561
Oligonucleotides		
TMEM150C Forward Primer 5′-GCGCTTCATCCAGCTAAAAC-3	Cosmo Genetech	N/A
TMEM150C Reverse Primer 5′-AAGTACGCCAGGAAGCACAT-3′	Cosmo Genetech	N/A

(*Continued on next page*)

Continued

REAGENT or RESOURCE	SOURCE	IDENTIFIER
Recombinant DNA		
mTTN3-pIRES2-acGFP	Hong et al., 2016	N/A
TMEM150C-siRNA1 5′-GCUUGUGGAUAGUGUACUU-3′	Bioneer	N/A
TMEM150C-siRNA2 5′-CUUGUGGAUAGUGUACUUU-3′	Bioneer	N/A
TMEM150C-siRNA3 5′-CAGAAGCUUCUGAAUAUCA-3′	Bioneer	N/A
Software and algorithms		
ImageJ	NIH	https://imagej.nih.gov/ij/
SigmaPlot 14.0	Systat	http://www.sigmaplot.co.uk/downloads/download.php
GraphPad Prism 8.0	GraphPad	https://www.graphpad.com/scientific-software/prism/
Zen 2.6	Zeiss	https://www.zeiss.com/microscopy/int/products/microscope-software/zen.html#downloads

RESOURCE AVAILABILITY

Lead contact

All requests should be forwarded and will be fulfilled by our Lead Contact, Uhtaek Oh (utoh@kist.re.kr) for additional information and resource requisitions.

Materials availability

This study did not generate new unique reagents.

Data and code availability

- All data reported in this paper will be shared by the lead contact upon request.
- This paper does not report original code.
- Any additional information required to reanalyze the data reported in this paper is available from the lead contact upon request.

EXPERIMENTAL MODEL AND SUBJECT DETAILS

Animals

All animal experiments were conducted in accordance with protocols approved by the Institutional Animal Care and Use Committee (IACUC) at the Korea Institute of Science and Technology and the ethical committee for animal welfare of the Seoul National University. *Ttn3*/TMEM150C KO C57BL/6J mice were provided by previous literature, (Hong et al., 2016). In order to prepare littermate WT and *Ttn3* KO mice for experimentations, $Ttn3^{+/-}$ mice were crossed with each other to give birth to $Ttn3^{+/+}$ and $Ttn3^{-/-}$ mice. All animals were housed, and lineages were maintained in Korea Institute of Science and Technology specific pathogen free animal facility. Food and water were provided *ad libitum*, lighting was scheduled at a 12 h light to dark cycle (07:00 ~19:00) and temperature and humidity were maintained around 22°C and 50%, respectively.

For intraperitoneal glucose and insulin tolerance tests, male mice around the ages 8 to 10 weeks after birth, were fasted and gave access to only water for 16 h and 6h, respectively. For glucose tolerance tests, male mice were injected with D-Glucose (2 g/kg body weight) (G8769, Sigma Aldrich) and blood samples were collected via tail cut at 0, 15, 30, 45, 60, and 120 min after intraperitoneal glucose injection. For insulin tolerance tests, male mice were injected with Humulin R (0.5 U/kg) (HI0210, Lilly) and blood samples were collected via tail cut at 0, 15, 30, 60, and 120 min after intraperitoneal Humulin R injection. Glucose levels were measured by OneTouch Ultra blood glucose meter (LifeScan, USA).

by OneTouch Ultra blood glucose meter (LifeScan, USA).

Cell Line Culture and Transfection

For cell line culture studies, pancreatic β-cell lines, NIT-1 (CRL-2055, ATCC), were cultured in the Rosewell park memorial institute (RPMI) 1640 medium (11875, GIBCO) supplemented with 10% fetal bovine serum (FBS) (26140, GIBCO), 100 U/ml penicillin, and 0.1 mg/ml streptomycin (15140, GIBCO). HEK293T (CRL-3216) cells were cultured in Dulbecco's modified eagle medium (DMEM) (11995, GIBCO) with 10% FBS, 100 U/ml penicillin, and 0.1 mg/ml streptomycin. Both cell lines were maintained under 37°C in 5% CO_2.

siRNA sequences were designed from the mouse TMEM150C sequence and synthesized by Bioneer (Korea). The sequences of three different siRNAs against TMEM150C used in calcium and insulin secretion assays were as follows: (siRNA1) 5′-GCUUGUG GAUAGUGUACUU-3′; (siRNA2) 5′-CUUGUGGAUAGUGUACUUU-3′; (siRNA3) 5′-CAGAAGCUUCUGAAUAUCA-3′. Negative control siRNAs provided by the manufacturer were used as control. The mixture of those three different siRNAs targeting TTN3 was transfected using RNAiMax (13778-030, Invitrogen) according to the manufacturer's protocol. Murine TTN3-pIRES2-AcGFP (Hong et al., 2016) plasmid was transfected with either FuGENE HD (E2311, Promega) or Lipofectamine 3000 (L3000015, Life Technologies) according to their respective manufacturers' protocol. Cells were processed and experimented after 48 h of transfection.

Primary culture of pancreatic β-cells

Male littermate WT or *Ttn3* KO mice were anesthetized using intraperitoneal injection of Zoletil 50 (25 mg/kg) and Rumpon (10 mg/kg) (Virbac). Hank's balanced salt solution (HBSS, 4 mL) with calcium (L0612, Biowest) containing 0.8 mg/ml collagenase P (11213865001, Roche) was injected into the common bile duct of mice in a 30G needle. The inflated pancreas was extracted with forceps and incubated for 15 min, while shaking every 2∼3 min, in a water bath at 37°C. The digested pancreas was put in a tube containing 40 mL of complete media (10% FBS in calcium-free HBSS(14175, GIBCO)) and centrifuged at 2000 rpm at 4°C for 3 min. The supernatant was removed, and the tissue pellet was washed by adding 40 mL of complete media and later centrifuged. The pellet was resuspended, filtered in a 500 μm mesh strainer, and centrifuged at 2000 rpm at 4°C for 3 min. After removing the supernatant, Biocoll (L6155, Biochrom) gradients with different densities (1.100, 1.085, 1.069, and 1.037) were added to the tissue pellet. The Biocoll mixture was centrifuged at 2000 rpm at 4°C for 20 min. Islets separated in densities between 1.085 and 1.069 were collected into serum, calcium-free HBSS, and centrifugated at 2000 rpm at 4°C for 1 min. After the supernatant was removed, the islets were resuspended in RPMI 1640 medium supplemented with 10% FBS, 100 U/ml penicillin, and 0.1 mg/ml streptomycin. Islets were sequentially isolated by two rounds of handpicking in a non-coated plate and cultured in non-coated wells filled with the RPMI 1640 media at 37°C and 5% CO_2. For patch-clamp and calcium imaging, islets were dispersed into single cells by trypsin digestion.

METHOD DETAILS

Immunohistochemistry

Pancreas tissue sections fixed in formalin were cut to 5 μm thickness onto glass slides before being embedded in paraffin. These sections were deparaffinized in xylene, then rehydrated with diluted concentrations of ethanol (100%, 95%, 80%, 75%) and deionized water for 3 minutes each. After antigen retrieval, sections were permeabilized with 0.2% PBST (phosphate-buffered saline containing 0.2% of Triton X-100) for 10 minutes and washed with PBS for 5 minutes three times. Sections were blocked with 3% bovine serum albumin (BSA) in 0.1% PBST for 30 min and sequentially washed with PBS for 3 minutes, three times each. Primary antibodies, such as insulin (mouse monoclonal, sc-8033, 1:500), glucagon (mouse monoclonal, G2654,1:2000), amylase (mouse monoclonal, sc-46657, 1:500), mPiezo1 (rabbit polyclonal, NBP1-78537, 1:200), and TTN3 (rabbit polyclonal, manufactured, 1:200) were added in the diluted blocking agent of 1% BSA in 0.02% PBST and incubated overnight in 4°C. Sections were then washed with PBS for 3 minutes, five times each, and stained with secondary antibodies conjugated to Alexa Flour 488 (A21202, 1:2000, Life Technology) and Alexa Flour 594 (A10072, 1:2000, Life Technology) in 1% BSA in 0.02% PBST for 40 minutes. Hoechst 33342 (H3570, 1:5000, Thermo Fisher Scientific) in PBS was used for nuclear staining. Images were then captured and observed using a Zeiss LSM700 confocal laser scanning microscope (Zeiss). Images were later analyzed by Zen 2.6 software (Zeiss).

RT-PCR

Total RNA was extracted using Easy-Spin™ Total RNA Extraction Kit (17221, Intron) according to the manufacturer's instructions. Thereafter, cDNA was synthesized from 1 μg total RNA using SuperScript III (18080, Invitrogen). RT-PCR was carried out using DreamTaq Green DNA Polymerase (EP0712, Thermo Scientific). Primers used for amplifying *Ttn3* were 5′-GCGCTTCATCCAGC TAAAAC-3′ and 5′-AAGTACGCCAGGAAGCACAT-3′.

Calcium Measurements

NIT-1 cells, grown in 96-well plates, were incubated with Fluo-4 NW (F36206, Invitrogen) for 1 h at 37°C and washed with isotonic (290 mOsm/kg) buffer solution. Fluo-4 NW was excited at 488 nm and emitted at 535 nm. The ratio of the fluorescence change, F/F0, was plotted to represent the changes in intracellular Ca^{2+} levels in response to 20 mM glucose or hypotonic (210 mOsm/kg) solution using SPARK 10M Multi reader (Tecan). Isolated pancreatic β-cells were loaded with Fura-2-AM (F1221, Molecular Probes) HBSS buffer (14175, GIBCO) at 37°C for 30 min. The cells were perfused with isotonic (290 mOsm/kg) buffer solution and changed with either high glucose (20 mM) or hypotonic (210 mOsm/kg) solutions. Depolarization of the cells with 30 mM KCl was used as a positive control at the end of the measurement. Fluorescent signals in single β-cells were imaged every 3 s via 340 nm excitation and 380 nm emission filters. All imaging data were collected by Meta Flour software (Molecular Devices). The ratios of fluorescence were calculated and analyzed using a digital fluorescence analyzer (MetaFlour, Molecular Devices) (Kim et al., 2007). For both measurements, isotonic (290 mOsm/kg) buffer solution contained (in mM): 85 NaCl, 5 KCl, 1.2 $MgCl_2$, 1.2 $CaCl_2$, 10 HEPES, 2.8 Glucose, and 100 D-mannitol (pH 7.4). Hypotonic (210 mOsm/kg) buffer contained (in mM): 85 NaCl, 5 KCl, 1.2 $MgCl_2$, 1.2 $CaCl_2$, 10 HEPES, and 2.8 Glucose

(pH7.4). High glucose (20 mM) buffer contained (in mM): 85 NaCl, 5 KCl, 1.2 $MgCl_2$, 1.2 $CaCl_2$, 10 HEPES, 20 Glucose, and 100 D-mannitol (pH7.4).

Electrophysiology

For voltage-clamp recordings in HEK293T or primary β-cells, intracellular potential (pipette voltage) was clamped at −60 mV. Whole cells were formed after rupturing the membrane under a glass pipette after gigaseal formation. The glass electrode resistance was 2-3 MΩ. The junctional potential was canceled to zero when the tip was immersed in the bath solution. Currents were amplified with an Axopatch 200B amplifier (Molecular Devices), filtered at 10 kHz (Low pass Bessel filter), and sampled at either 5 or 10 kHz (Digidata 1440A, Molecular Devices). For current-voltage relationships, voltage ramps from −80 mV to + 80 mV were applied for 150 ms during the hypotonic solution challenge. For current-clamp recordings, bias current was not injected. Data were analyzed by pClamp software version 10.0 (Molecular Devices). Resting membrane potentials were measured as averaged membrane potential for 10 s before applying high glucose or hypotonic stimulations. The number of action potentials, firing rates, peak voltage, and amplitude were measured as baseline subtracted averages during the firing activity of the cell.

Solutions

For recording current responses in the primary β-cells and in HEK293T cells, the basal extracellular solution contained (in mM): 90 NaCl, 2 KCl, 1 $MgCl_2$, 1 $CaCl_2$, 10 HEPES, and 90 D-mannitol (pH 7.2), while hypotonic solution contained the same components with the exemption of D-Mannitol. The intracellular solution contained (in mM): 130 CsCl, 2 $MgCl_2$, 10 HEPES, 2 Mg-ATP, 0.2 Na-GTP and 30 D-mannitol (pH 7.2). To block Cl^- current, Na-gluconate solution was used; the isotonic (287 mOsm/kg) bath solution contained (in mM): 100 Na-Gluconate, 2 $CaCl_2$, 10 HEPES, 90 D-Mannitol (pH 7.21). The hypotonic solution contained the same components with the exemption of D-Mannitol. The glucose concentration for standard bath solution was either 0 mM or 2.8 mM, whereas high glucose stimulation was by 20 mM Glucose. Osmolality was also adjusted with mannitol for 20mM glucose stimulation. The intracellular solution (287 mOsm/kg) contained (in mM): 100 Na-Gluconate, 10 HEPES, 90 D-Mannitol (pH 7.21). For current-clamp recordings, the isotonic (280 mOsm/kg) bath solution consisted of (in mM): 85 NaCl, 5 KCl, 10 HEPES, 1.2 $MgCl_2$, 1.2 $CaCl_2$, and 80 D-mannitol (pH 7.3 with NaOH). For hypotonic (210 mOsm/kg), the solution contained the same components with the exemption of D-Mannitol. The glucose concentration for standard bath solution was either 0 mM or 2.8 mM, whereas high glucose stimulation was by 20 mM Glucose. The intracellular solution contained (in mM): 138 KCl, 10 NaCl, 1 Mg Cl2, 10 HEPES, 10 EGTA (pH 7.3 with KOH), 5 ATP, and 0.1 GTP.

Mechanical Stimulation

Mechanical stimulations were carried out as described previously (Hong et al., 2016). Briefly, a fire-polished thin glass electrode (tip diameter 3–4 μm) was positioned at an angle of ∼50° to the cell surface. Controlled by a micromanipulator (Nano-controller NC4; Kleindiek Nanotechnik), the glass probe moved downward in a series of mechanical steps in 1 μm during the ramp segment of the command. The typical duration of the mechanical stimulation was 600 ms.

Insulin Assay

NIT-1 cells and pancreatic islets were cultured in 6-well coated and non-coated plates, respectively, and washed twice with glucose-free HEPES-balanced Krebs-Ringer-Bicarbonate buffer (KRBH) and then pre-incubated with glucose-free Rosewell Park Memorial Institute 1640 medium for 2 h at 37°C and in 5% CO_2. Cells were then pre-incubated in KRBH buffer for 1 h at 37°C and in 5% CO_2. After removal of the pre-incubation solution, the cells were incubated in KRBH buffer containing low (2.5 mM) glucose or high (20 mM) glucose solution for 1 h. Incubation media was collected, and the amount of insulin was measured using ELISA (80-INSMS-E01, ALPCO). For insulin content measurements, cold 0.2 M HCl in 95% ethanol was added to the islets after glucose stimulation. After brief sonication, an additional 0.2 M HCl in 95% ethanol was added and chill-incubated while shaking overnight. After the removal of the supernatant, 0.2 M NaOH was applied for neutralization. The mixture was then centrifuged at 12,000 rpm at 4°C, and the supernatant was collected for measuring insulin levels with Ultra Sensitive Mouse Insulin ELISA Kit (90080, Crystal Chem). The insulin levels were adjusted and normalized from the total cellular protein of cell lysate. The measurement from the plate of cells with the control medium stimulated by low glucose was considered as 0% of glucose-stimulated insulin secretion. For serum insulin measurement, blood samples were collected via tail cut at 0, 10, 20, and 30 min after intraperitoneal glucose injection (2 g/kg body weight). After centrifugation at 2500 rpm, Ultra Sensitive Mouse Insulin ELISA Kit was used to determine the serum insulin values.

β-cell mass measurement

Murine pancreases were extracted from anesthetized littermate WT and *Ttn3* KO mice and fixated in 4% paraformaldehyde in 4°C. The pancreas weight was measured after removing the excess fixation agent. Pancreas tissues were embedded in paraffin and cut in 40 μm thickness. After deparaffinization, DAB staining with insulin (mouse monoclonal, sc-8033, 1:500) antibody onto pancreas sections was performed according to the manufacturer protocol. Insulin-positive stained areas and total pancreas areas were observed through an epifluorescence microscope and measured by ImageJ software (NIH). β-cell mass was then calculated through the multiplication of the relative insulin-positive area by its corresponding pancreas weight.

QUANTIFICATION AND STATISTICAL ANALYSIS

Transcript Level Quantification

Quantifying the specified region of interest was first drawn in RT-PCR blot images and mean intensities were measured through ImageJ(NIH). Target expression levels were normalized to the measured intensity of the housekeeping gene, GAPDH.

Statistical Analysis

Data were processed and analyzed with Prism 7 (GraphPad) and SigmaPlot 14.0 (Systat). Data and error bars are presented as means ± SEM ''n'' indicates the number of replicate samples experimented. Comparisons between groups were performed by two tailed unpaired Student's t test. Multiple comparisons of the means were analyzed with one-way ANOVA with Tukey's post hoc tests. P values less than 0.05 are considered significant (*$p < 0.05$, **$p < 0.01$, ***$p < 0.001$).

Cell Reports, Volume *37*

Supplemental information

Tentonin 3/TMEM150C regulates glucose-stimulated insulin secretion in pancreatic β-cells

Jungwon Wee, Sungmin Pak, Tahnbee Kim, Gyu-Sang Hong, Ji Seon Lee, Jinyan Nan, Hyungsup Kim, Mi-Ock Lee, Kyong Soo Park, and Uhtaek Oh

Supplementary Information

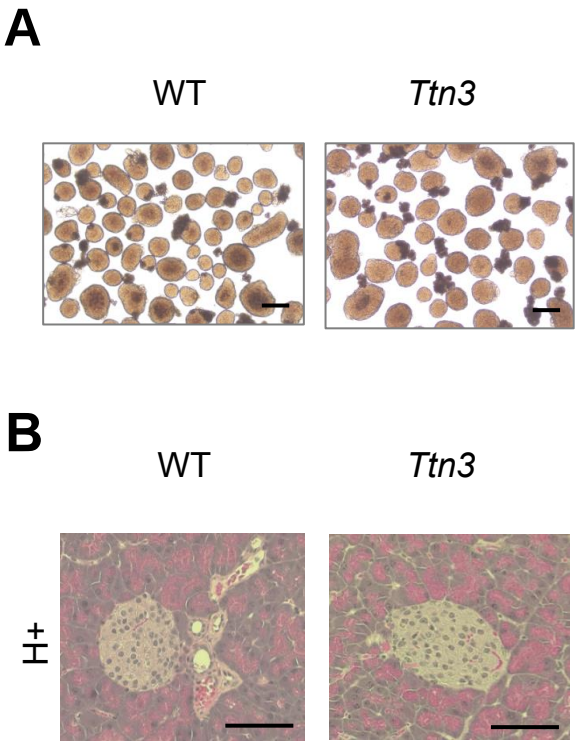

Figure S1. Islet morphology of WT and *Ttn3* KO mice. Related to Figure 6

A. Representative photographs of freshly isolated pancreatic islets from WT (left) and *TTN3* KO (right) mice. Scale bars: 200 μm.

B. Pancreatic islets from WT and *Ttn3* KO mice stained with hematoxylin-eosin. Scale bars: 200 μm.

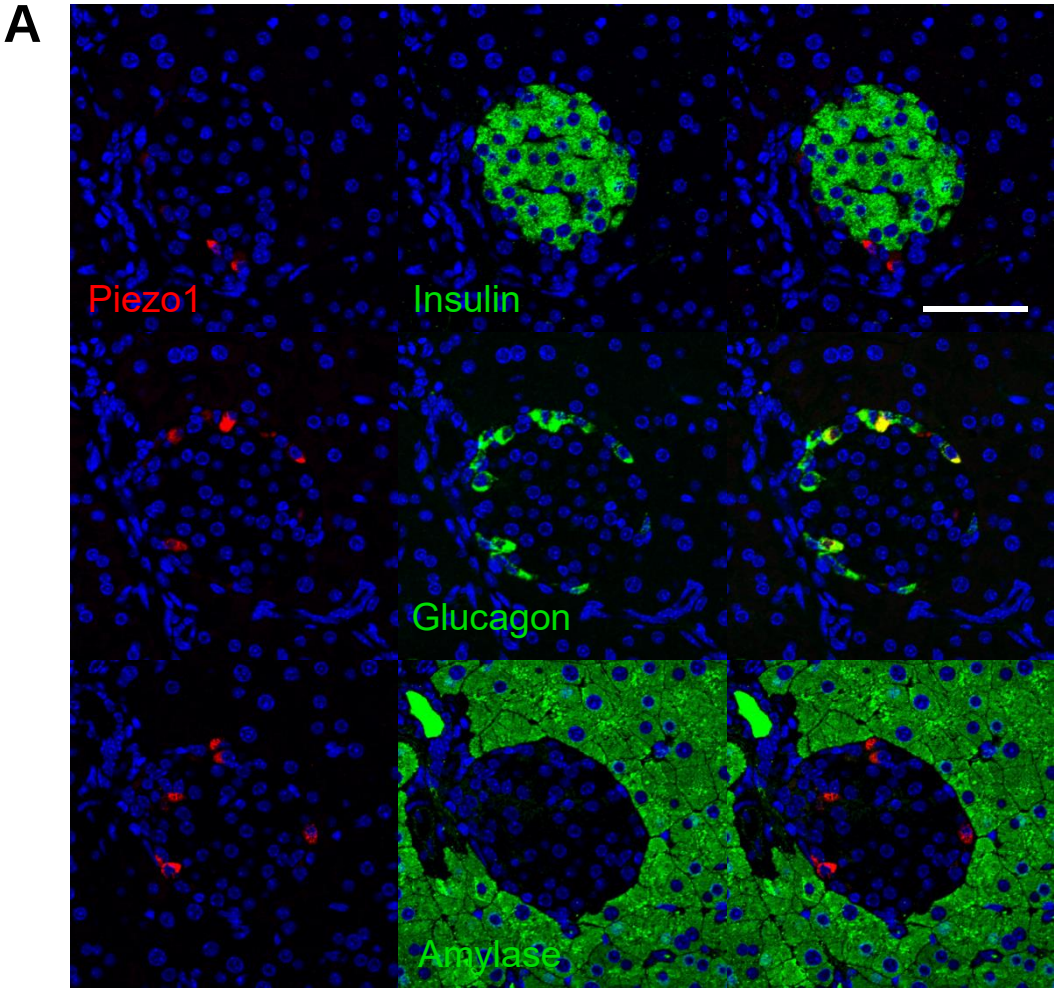

Supplementary Figure 2

Figure S2. Expression of Piezo1 in mouse pancreatic islets. Related to Figure 1 and Discussion.

Immunofluorescence staining of Piezo1 (red) and insulin (green), glucagon (green) or amylase (green) in mouse pancreas sections. Scale bars: 50 μm.